Angiogenesis (2019) 22:441–455
https://doi.org/10.1007/s10456-019-09669-x

ORIGINAL PAPER

Cancer stem cells contribute to angiogenesis and lymphangiogenesis in serous adenocarcinoma of the ovary

Syama Krishnapriya[1] · Chirukandath Sidhanth[1] · Pacharla Manasa[1] · Smarakan Sneha[1] · Sadhanandhan Bindhya[1] · Rohit P. Nagare[1] · Balaji Ramachandran[2] · Pushpa Vishwanathan[3] · Kanchan Murhekar[4] · Sundersingh Shirley[4] · Trivadi Sundaram Ganesan[1]

Received: 28 February 2019 / Accepted: 15 May 2019 / Published online: 3 June 2019

Abstract

The origin of blood and lymphatic vessels in high-grade serous adenocarcinoma of ovary (HGSOC) is uncertain. We evaluated the potential of cancer stem cells (CSCs) in HGSOC to contribute to their formation. Using spheroids as an in vitro model for CSCs, we have evaluated their role in primary malignant cells (PMCs) in ascites from previously untreated patients with HGSOC and cell lines. Spheroids from PMCs grown under specific conditions showed significantly higher expression of endothelial, pericyte and lymphatic endothelial markers. These endothelial and lymphatic cells formed tube-like structures, showed uptake of Dil-ac-LDL and expressed endothelial nitric oxide synthase confirming their endothelial phenotype. Electron microscopy demonstrated classical Weibel–Palade bodies in differentiated cells. Genetically, CSCs and the differentiated cells had a similar identity. Lineage tracking using green fluorescent protein transfected cancer cells in nude mice confirmed that spheroids grown in stem cell conditions can give rise to all three cells. Bevacizumab, a monoclonal antibody that targets vascular endothelial growth factor inhibited the differentiation of spheroids to endothelial cells in vitro. These results suggest that CSCs contribute to angiogenesis and lymphangiogenesis in serous adenocarcinoma of the ovary, which can be inhibited.

Keywords Cancer stem cells · Endothelial cells · Pericytes · Lymphangiogenesis · Bevacizumab · Serous adenocarcinoma of ovary

Introduction

Over the last few years, tumour vascularization has been demonstrated to occur through angiogenesis, vasculogenesis, vasculogenic mimicry, vascular co-option and intussusceptive angiogenesis [1]. However, the origin of the component cell types of a blood vessel such as endothelial cells (ECs) and pericytes is unknown [2]. CSCs have been reported to be one of the reasons for recurrence of the tumour as they are resistant to conventional chemotherapy and other targeted therapies [3]. Recently, it has been demonstrated that a proportion of ECs arise from CSCs in glioblastoma (GBM) [4, 5]. However, it was demonstrated by another group that the glioblastoma stem-like cells give rise to pericytes and not ECs [6]. This route of tumour vascularization via CSCs has been convincingly shown only in GBM whereas there are little data in other types of cancer [7, 8]. The origin of ECs and other stromal cells, which form a tumour blood vessel in other tumour types, remains to be determined. Lymphangiogenesis is the development of new lymph vessels from pre-existing lymph vessels, which contribute to the metastasis of the tumour [9]. However, the origin of lymphatic endothelial cells (LECs) in a tumour has also not been evaluated. HGSOC accounts for the majority of deaths due to ovarian cancer. It is diagnosed mostly at the

Electronic supplementary material The online version of this article (https://doi.org/10.1007/s10456-019-09669-x) contains supplementary material, which is available to authorized users.

✉ Trivadi Sundaram Ganesan
tsganesan@gmail.com; ts.ganesan@cancerinstitutewia.org

[1] Laboratory for Cancer Biology, Departments of Medical Oncology and Clinical Research, Cancer Institute (WIA), 38, Sardar Patel Road, Guindy, Chennai 600036, India

[2] Department of Molecular Oncology, Cancer Institute (WIA), Chennai 600036, India

[3] Department of Electron microscopy, Cancer Institute (WIA), Chennai 600036, India

[4] Department of Pathology, Cancer Institute (WIA), Chennai 600036, India

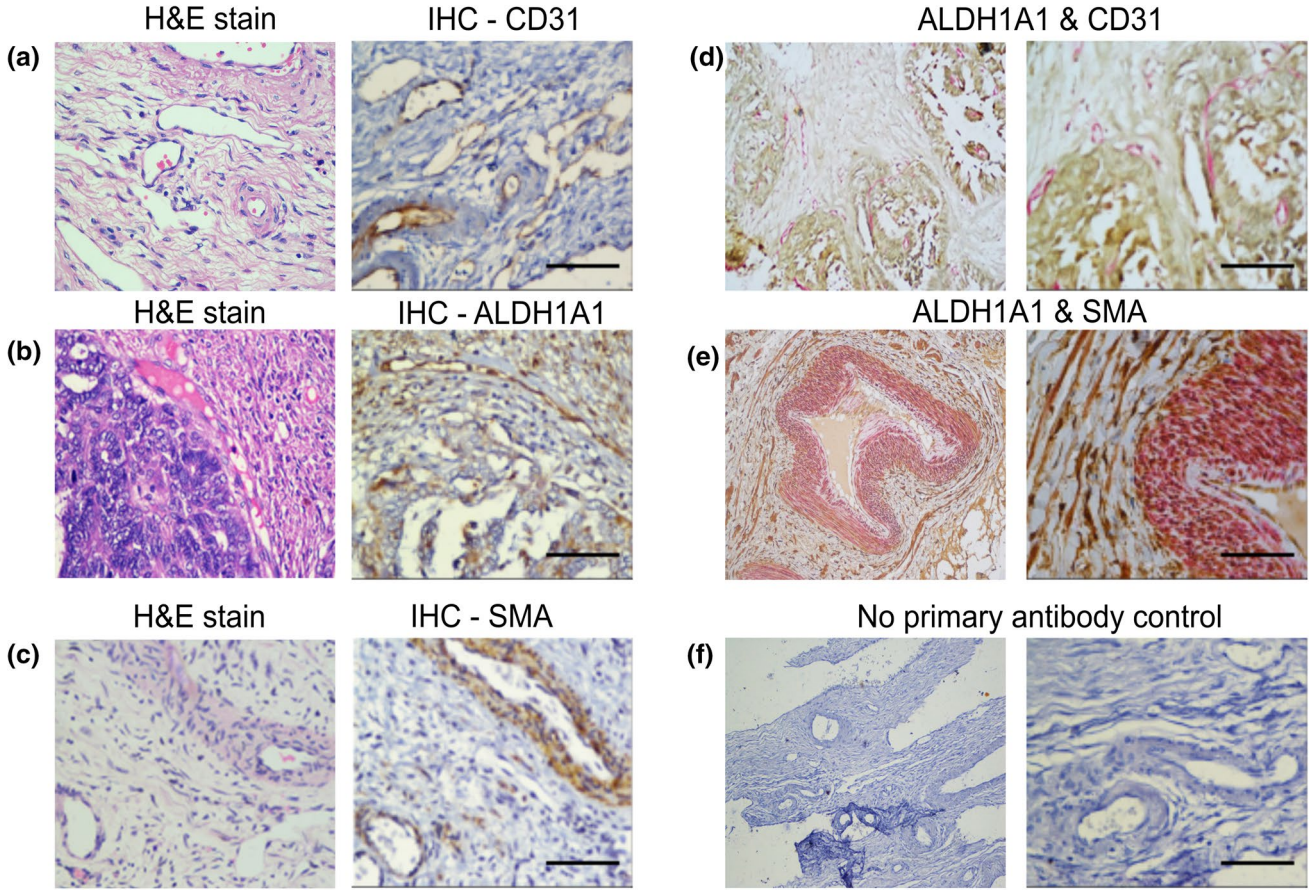

Fig. 1 Expression of ALDH1A1, CD31 and SMA by IHC in HGSOC. Representative images showing the expression of **a** CD31, **b** ALDH1A1 and **c** SMA in paraffin sections of a tumour (HGSOC). H&E stained sections are shown in the left panels of (**a**–**c**). Double IHC of ALDH1A1 (brown) with **d** CD31 (pink) and **e** SMA (pink), **f** no primary antibody control. Scale bar: 10 µm

advanced stages and the outcome can be improved. Hence, our objective was to study if the origin of ECs, pericytes and LECs in HGSOC is from CSCs.

Results

Proximity of blood vessels to CSCs

We have evaluated the localization of blood vessels and CSCs in ovarian tumours by double immunohistochemistry (IHC) (Fig. 1a–c). The CSCs were identified by their expression of ALDH1A1, as there is no conclusive evidence for a unique marker for ovarian CSCs [10]. The co-immunostaining of ALDH1A1 and CD31 showed that the blood vessels lie adjacent to CSCs in HGSOC (Fig. 1d). The pink stain represents the CD31 positive blood vessels and brown stain indicates the ALDH1A1 positive CSCs. The proximity of blood vessels to CSCs was observed in different specimens of HGSOC. The double immunostaining of ALDH1A1 and SMA showed that ALDH1A1 and SMA are co-expressed in tumours of HGSOC (Fig. 1e). Tissue incubated with no primary antibody (negative control) had no stained cells (Fig. 1f).

Expression of endothelial markers in cells from malignant ascites

PMCs from previously untreated patients with HGSOC were used for our experiments. CD31, CD105, CD144 are well known surface markers of blood vessels [11]. The Aldefluor assay that identifies ALDH1A1 high cells was used simultaneously with antibodies against endothelial markers (Fig. 2a) and evaluated by flow cytometry (FC). Interestingly, using the ALDH1A1 functional assay together with an analysis of expression of endothelial markers, CD31, CD105, CD144 and CLEC14A, we identified a small population of cells (mean < 1%) co-expressing both ALDH1A1 and an endothelial marker (Table S1).

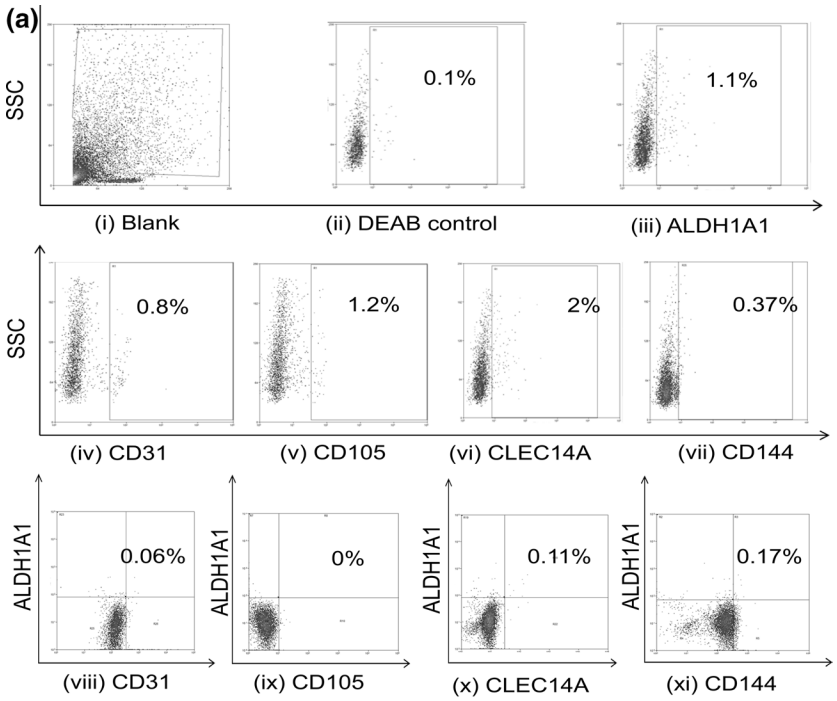

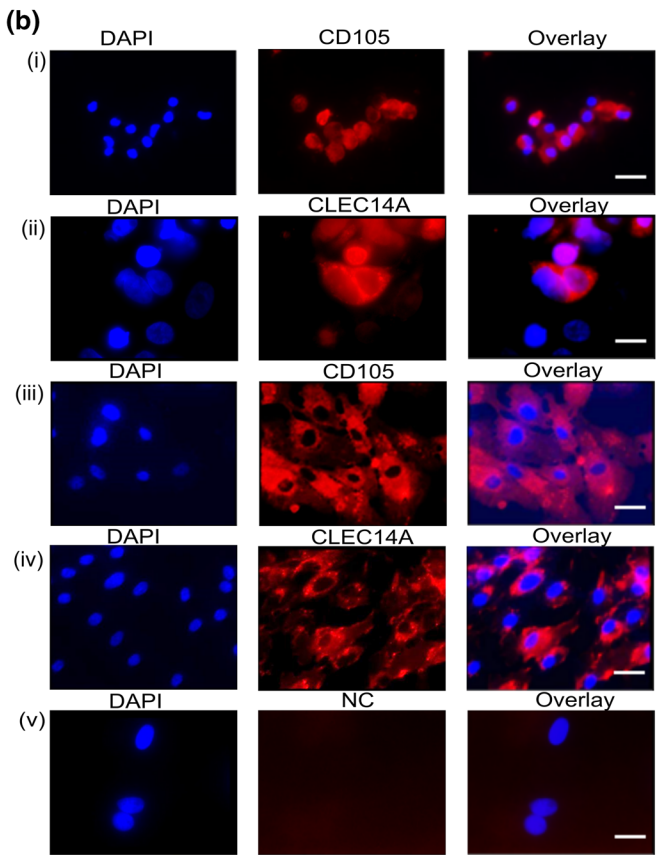

Fig. 2 Expression of endothelial markers and ALDH1A1 in PMCs. **a** PMCs were analysed for expression of endothelial markers and CSCs by flow cytometry (FC). Representative FC plot for Aldefluor assay—(i) unstained, (ii) DEAB control and (iii) ALDH1A1 (top panel), Expression of endothelial markers, (iv) CD31, (v) CD105, (vi) CLEC14A and (vii) CD144 (middle panel) and Co-expression of ALDH1A1 and (viii) CD31, (ix) CD105, (x) CLEC14A and (xi) CD144 (bottom panel). All antibodies were labelled with respective fluorochromes and the cells were also labelled with isotype specific antibody control for each fluorophore and the fluorescence was less than 0.5% (data not shown). **b** Expression of (i) CD105 and (ii) CLEC14A in PMCs cultured in EGM. Expression of (iii) CD105 and (iv) CLEC14A in HUVECs. (v) No primary antibody control (NC). Scale bar: 50 µm. Objective EC Plan-Neofluar 40X/0.75, Carl Zeiss Axio imager 3.1. **c** Representative FC plots showing the expression of CD105 (secondary antibody labelled with AF647), CLEC14A (secondary antibody labelled with PE) and co-expression of CD105 and CLEC14A in spheroids and cells cultured in EGM. Statistical analysis of the difference in expression of each marker (right panel) is shown graphically (Wilcoxon signed rank test). **d** PMCs were sorted for ALDH1A1+ cells by Aldefluor assay and were cultured for 7 days in EGM. Flow cytometry analysis of these cells with CD31 PE and CD105 AF647 is shown

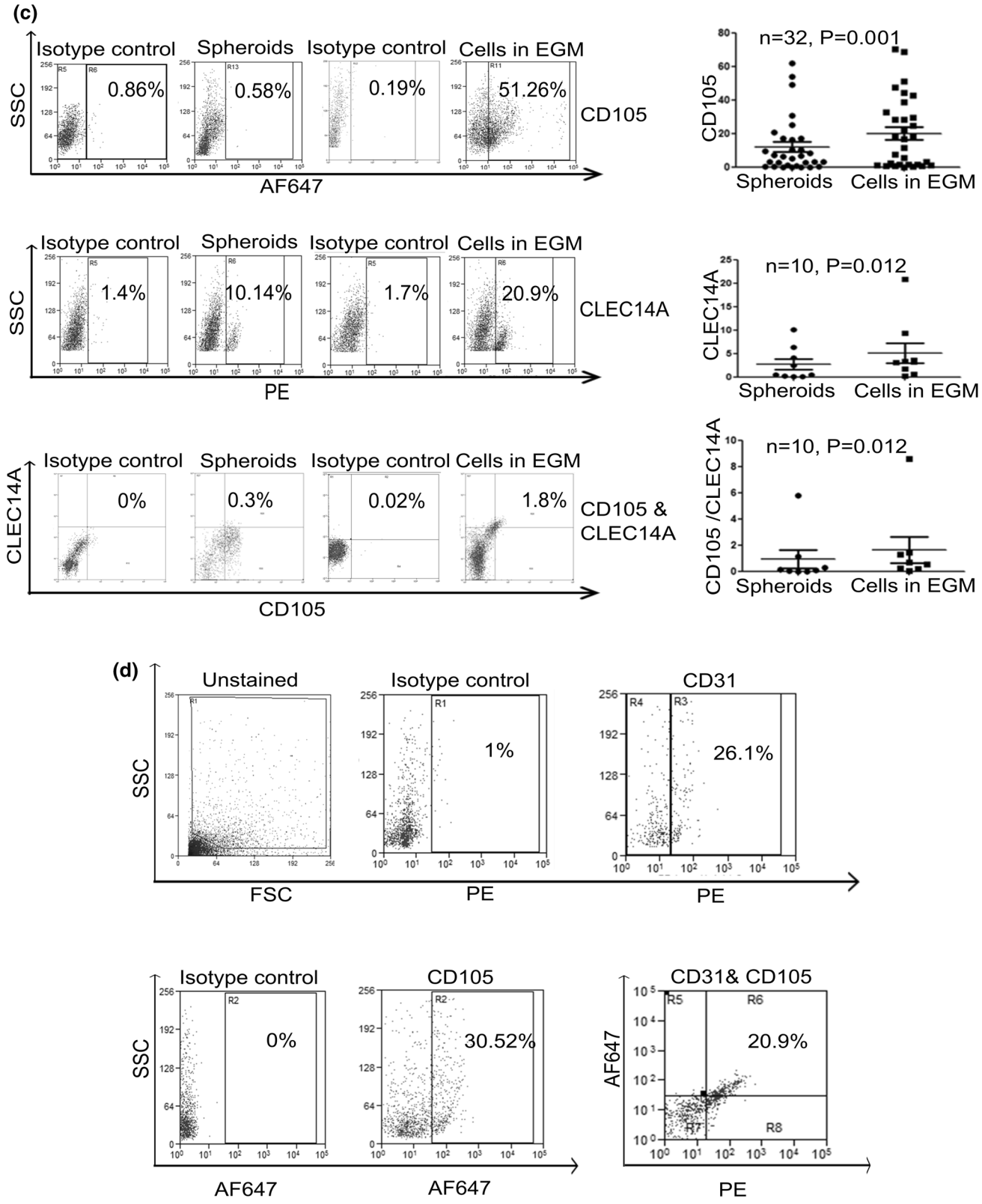

Fig. 2 (continued)

ECs are derived from CSCs in vitro

Spheroids formed by PMCs were grown under stem cell medium (SCM) for 1 to 2 weeks initially and dispersed to single cells and were cultured in endothelial growth medium (EGM) for 7 days. The immunostaining of cells grown in EGM by CD105 and CLEC14A antibodies showed that they express both markers (Fig. 2b). Human Umbilical Vein ECs (HUVECs) served as control. PMCs (n = 32) were grown initially under 3D conditions for 7 days to form spheroids and further grown in EGM for 7 days. Cells grown under SCM and EGM were evaluated for the expression of CD105 and CLEC14A by FC (Fig. 2c). Cells grown in EGM showed a significantly higher expression of CD105 ($P = 0.001$) and CLEC14A ($P = 0.012$). The combined expression of both markers was also significantly higher ($P = 0.01$) in cells grown in EGM (Table S2a). In addition, PMCs when sorted for ALDH1A1+ cells by FACS and cultured in EGM, showed expression of both CD31 and CD105 (Fig. 2d). To confirm our observations, the FC analysis was performed simultaneously in a single tube using antibodies against CD31, CD105, CD144 and CLEC14A. All the markers showed an increase in cells grown in EGM compared to spheroids in at least 4 out of 5 samples (data not shown).

Functional analysis of ECs derived from CSCs

The classical assay used to evaluate the functional property of ECs is the uptake of Dil-labelled acetylated low density lipoprotein (Dil-ac-LDL) [12]. The PMCs, when cultured in EGM, showed uptake of Dil-ac-LDL (Fig. 3a). Secondly, we evaluated for expression of eNOS [13]. The immunofluorescence of cells cultured in EGM showed expression of eNOS (Fig. 3b). In the third assay, we demonstrated that PMCs cultured in EGM formed tube-like structures when grown in 3D conditions after 24 h of seeding (Fig. 3c) [14]. All these assays were performed after verifying that cells grown in EGM expressed endothelial specific markers (data not shown). HUVECs served as the control for all the three assays.

Ultra-structure of ECs derived from CSCs

The cells cultured in EGM from the ovarian cancer cell lines, CAOV3 and OVCAR3 (both derived from patients with HGSOC), showed characteristic features of ECs when observed under a transmission electron microscope (TEM) similar to that of HUVECs. We observed the presence of Weibel–Palade bodies (WPBs), the storage granules of von Willebrand factor (vWF), which is one of the reported features of ECs [15–17]. We could also identify the gap junctions between two cells (Fig. 3d) which are also a special characteristic of ECs [18].

Co-expression of CCNE1 and endothelial marker, CD31 in HGSOC

Cyclin E1 (CCNE1) is localized to chromosome 19q12 and has been shown to be amplified in malignant cells of HGSOC [19]. It is reported to be amplified and overexpressed in 24.5% (146/594 cases) of patients with HGSOC [20]. We selected formalin fixed paraffin embedded (FFPE) sections of CCNE1 expressing tumours ($n = 5$) for IHC. To demonstrate if blood vessels are derived from malignant cells, double IHC was performed in these tumours. CCNE1 was primarily expressed in the nuclei and CD31 + ECs also co-expressed CCNE1 in their nuclei. The results showed that a proportion of ECs (~25%) expressing CD31 also expressed CCNE1 (Fig.S1).

Are pericytes derived from ovarian CSCs?

Spheroids formed by PMCs ($n = 10$) were grown in DMEM supplemented with 10% FBS for 6 days. Pericytes were identified by their expression of desmin and Smooth muscle actin (SMA). The FC analysis showed that the expression of both desmin and SMA was increased (Fig. 4a, $P = 0.03$ and $P = 0.017$, respectively; Table S2b). CCNE1 is amplified in HGSOC and it can be demonstrated by FISH using specific probes. We performed immuno-FISH with a spectrum green labelled CCNE1 specific probe and an antibody against SMA in formalin fixed sections of HGSOC. The amplification of CCNE1 in SMA+ pericytes confirms that they are genetically identical to the ovarian tumour cells (Fig. 4b). By Immuno-FISH and double IHC, we demonstrated that CCNE1 was predominantly localized to the nucleus in cells positive for either SMA or desmin (Fig. 4b).

Lymphatic endothelial cells (LECs) are derived from ovarian CSCs in vitro

VEGF-C is the ligand for LECs and signals via vascular endothelial growth factor receptor 3 (VEGFR3) [21, 22]. Spheroids formed by PMCs ($n = 10$) cultured in EGM along with VEGF-C (100 ng/ml), were evaluated for the expression of VEGFR3 by FC. Cells grown in EGM with VEGF-C, showed increased expression of VEGFR3 compared to spheroids in all the samples (Fig. 5a–c). The mean difference in expression of VEGFR3 was significant ($P = 0.028$) (Table S2c). In addition, the dispersed cells cultured in 3D conditions with EGM containing VEGF-C, formed tube-like structures after 24 h of seeding (Fig. 5d, e).

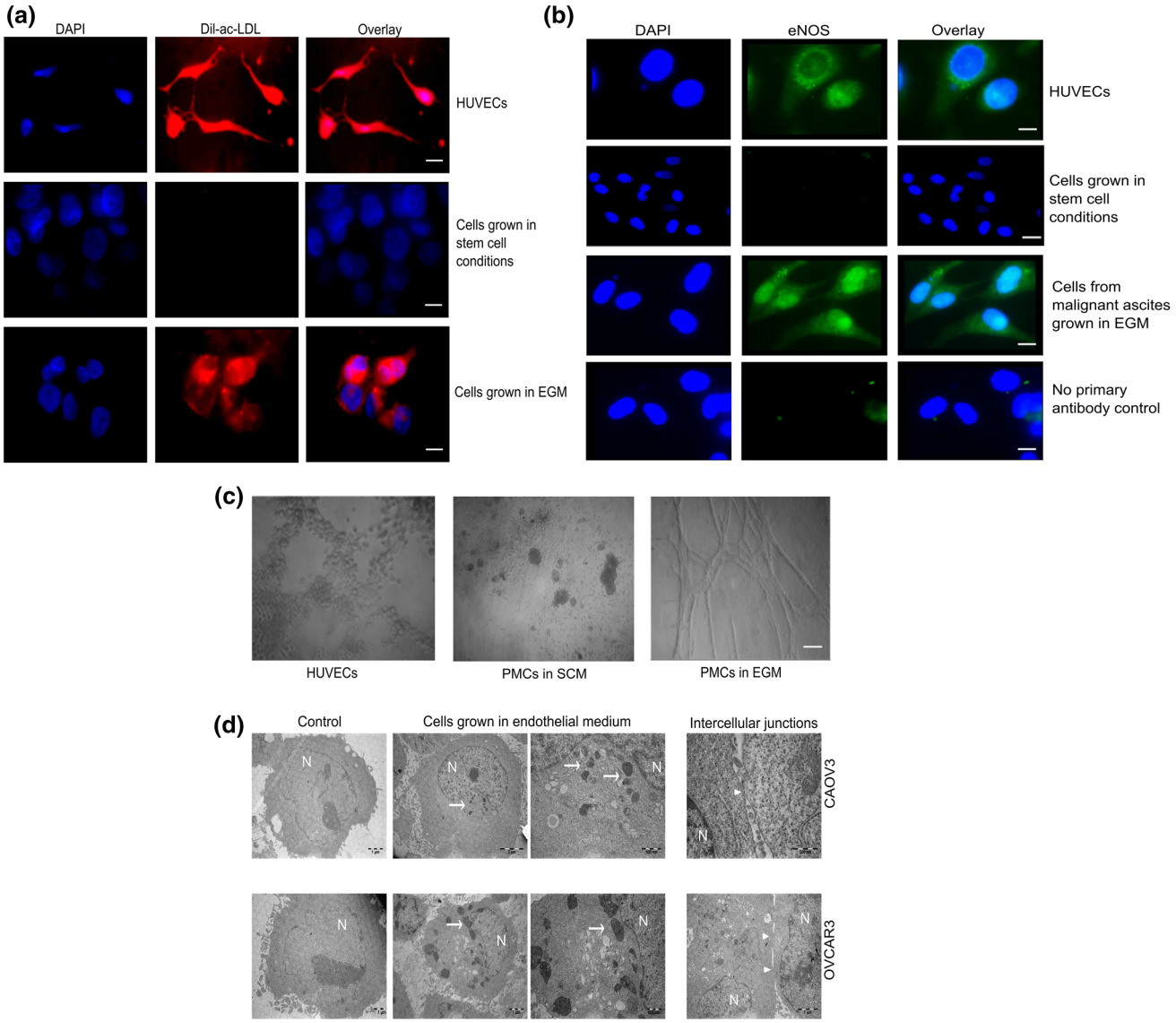

Fig. 3 Functional analysis and ultra-structure of CSC derived ECs. Cells were incubated with 1 µg/µl of Dil-ac-LDL for 4 h at 37 °C. **a** Uptake of Dil-ac-LDL by HUVECs (top), PMCs grown in SCM (middle) and EGM (bottom), Scale bar: 20 µm. **b** Expression of eNOS by HUVECs, PMCs grown in SCM and EGM are shown, Scale bar: 20 µm. Objective EC Plan-Neofluar 40X/0.75, Carl Zeiss Axio imager 3.1. **c** Formation of tube-like structures by HUVECs, PMCs grown in SCM and EGM are shown, Scale bar: 50 µm. **d** Ultra-structure of cells cultured in EGM was visualized by TEM. Weibel–Palade bodies (white arrows), and inter-cellular junctions (arrow heads) were observed in CAOV3 and OVCAR3 cell lines. N represents nuclei

Ovarian CSCs support tumour angiogenesis and lymphangiogenesis in vivo

We transfected cells from two cell lines, CAOV3 and OVCAR3, with GFP vector (pLKO.1-puro-CMV-TurboGFP, Sigma) to enable tracking of these cells. These stably GFP transfected cells were grown in SCM to form spheroids which were injected subcutaneously to the right flank of nude mice. Tumours were formed in mice injected with spheroids from CAOV3 ($n = 3/4$) and OVCAR3 ($n = 3/6$) cells, respectively. Hematoxylin and eosin (H&E) staining of the frozen sections from xenograft tumours formed by spheroids from CAOV3 and OVCAR3 cells showed the histology of adenocarcinoma (Fig. 6a). The immunostaining of the same frozen tumour sections with CD31 antibody showed the presence of 10% of CD31+ blood vessels co-expressing GFP (Fig. 6b).

The immunofluorescence of the same xenograft tumour (frozen) sections with SMA antibody, showed the co-expression of GFP in SMA+ pericytes (Fig. 6c). This suggested that a proportion of pericytes (20–25%) was derived from GFP+ ovarian CSCs.

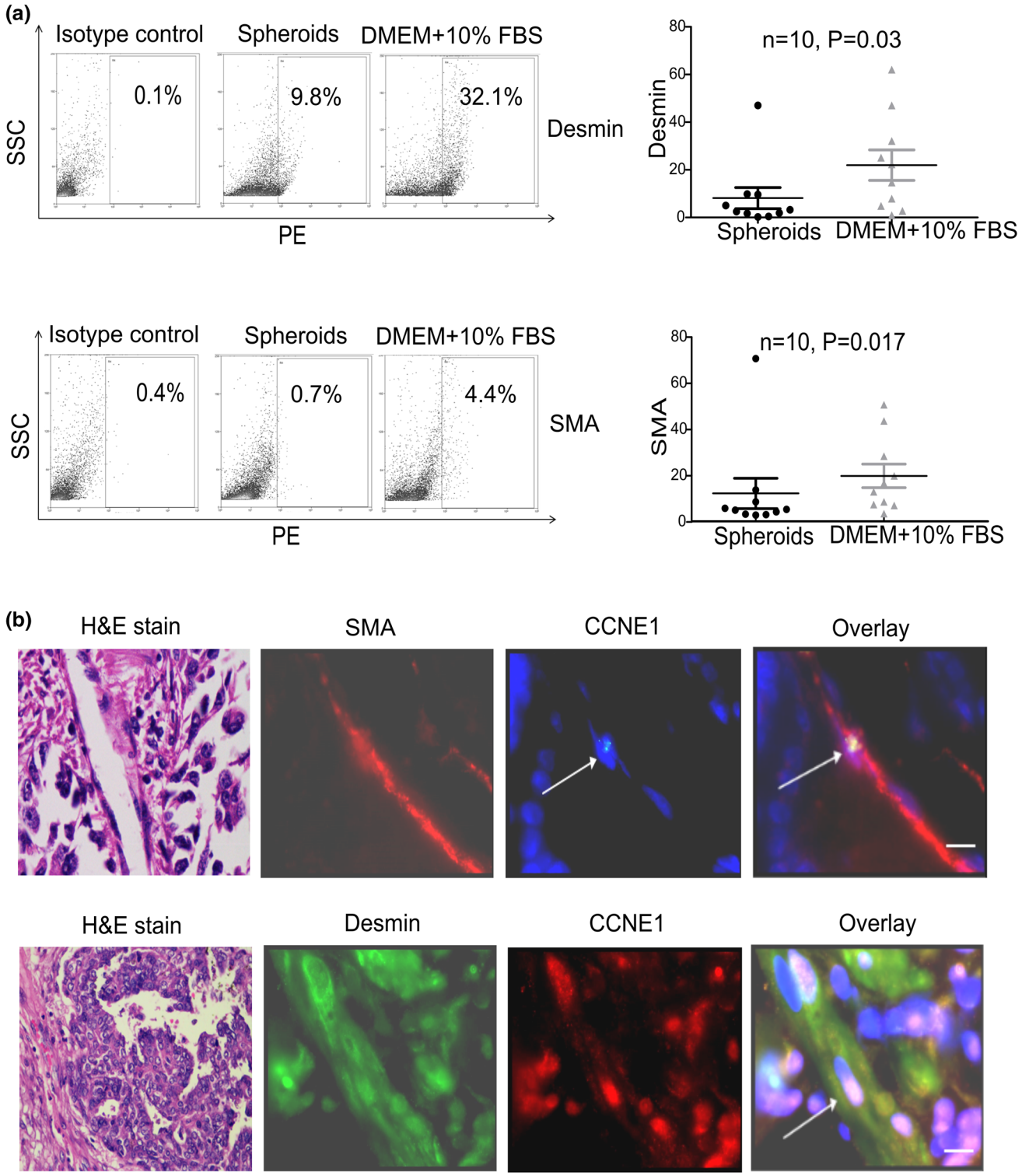

Fig. 4 CSCs in HGSOC give rise to pericytes in vitro. **a** Representative FC plots showing the expression of desmin and SMA in PMCs. Statistical analysis of the difference in expression of desmin and SMA is shown graphically (Wilcoxon signed rank test). **b** Immuno-FISH of SMA and CCNE1 probe in a primary ovarian tumour. Arrow shows the CCNE1 amplification in the nucleus of a SMA+ pericyte (top panel). Co-expression of CCNE1 and desmin in primary ovarian tumour by IHC (bottom panel). Anti-rabbit PE secondary antibody was used for CCNE1 (red fluorescence) and anti-mouse FITC was used for desmin (green fluorescence). Dual staining of CCNE1 and desmin in a blood vessel was observed (white arrows), Scale bar: 50 µm. Objective EC Plan-Neofluar 100X/1.3 oil, Carl Zeiss Axio imager 3.1

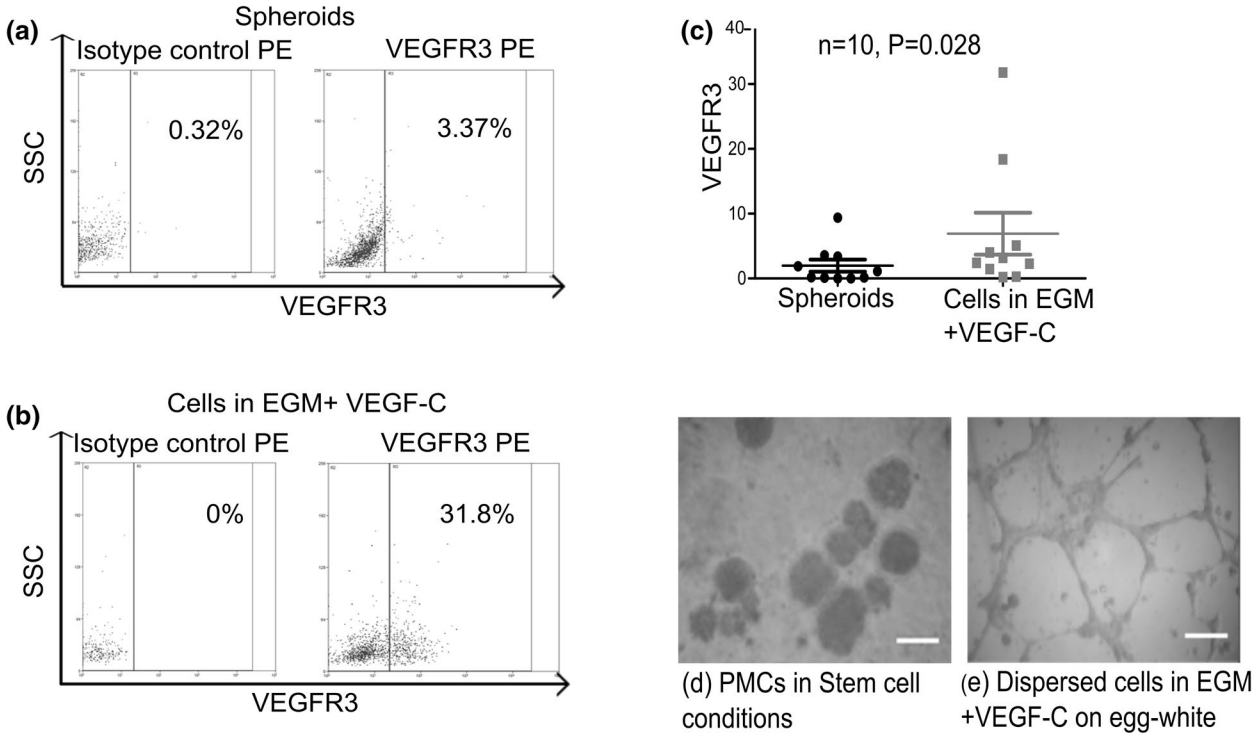

Fig. 5 Lymphatic endothelial differentiation of PMCs from malignant ascites. Representative FC analysis of PMCs with VEGFR3 antibody in **a** spheroids and **b** cells in EGM with VEGF-C. Statistical analysis of the difference in expression of **c** VEGFR3 shown graphically (Wilcoxon signed rank test). PMCs grown in **d** SCM and **e** in EGM with VEGF-C (100 ng/ml). Tube-like structures were formed by PMCs when grown in EGM containing VEGF-C (**e**), scale bar: 50 µm

On immunofluorescence with VEGFR3 antibody on the xenograft tumour (frozen) sections, co-expression of GFP in VEGFR3+ vessels (5–10%) was observed (Fig. 6d).

Bevacizumab inhibits the differentiation of ovarian CSCs to ECs

The spheroids from PMCs ($n=10$) were treated with and without Bevacizumab (1 µg/µl) in EGM for 7 days. On FC analysis, the expression of CD105 and CLEC14A was decreased in all the samples when treated with Bevacizumab (Table S3). Although individually the decrease in expression of either CD105 or CLEC14A was not significant, the cells expressing both were significantly reduced following treatment with Bevacizumab ($P=0.04$). (Fig. 7a).

Further, cells from spheroids formed by CAOV3 cells were grown in EGM with and without Bevacizumab (1 µg/µl). The expression of eNOS was significantly increased when cells are grown in EGM as compared to spheroids in SCM, which was inhibited in the presence of Bevacizumab (Fig. 7b).

Spheroids from CAOV3 cells were cultured in EGM in either the presence or absence of Bevacizumab or cediranib (VEGFR2 inhibitor). We examined primarily the MAP kinase, PI-3 kinase/AKT and STAT3 pathways. As an additional control, spheroids grown in SCM were starved for 48 h. In CAOV3, there was no expression of pERK in spheroids grown in SCM, whereas it was expressed in cells cultured in EGM. There was a reduction in the expression of the pERK upon treatment with Bevacizumab and cediranib. There was weak expression of pAKT in the cells cultured in EGM as well as cells treated with cediranib and no expression of pAKT in cells treated with Bevacizumab. Interestingly, there was a reduction in the expression of pSTAT3 on treatment with Bevacizumab and cediranib (Fig. 7b).

Discussion

Angiogenesis is an important hallmark of cancer [23]. The correlation of vascular density in primary ovarian tumours with outcome has been conflicting [24]. Despite this, recent randomized trials have shown that anti-angiogenic drugs significantly improve disease free survival [25].

Usually, tumour cells get their nutrients and oxygen through neighbouring stroma. However, the cells in the inner core of the tumour are under hypoxia and they use other mechanisms of vascularization as previously described [2, 26]. There is controversy in glioma whether CSCs give rise to ECs or pericytes [2].

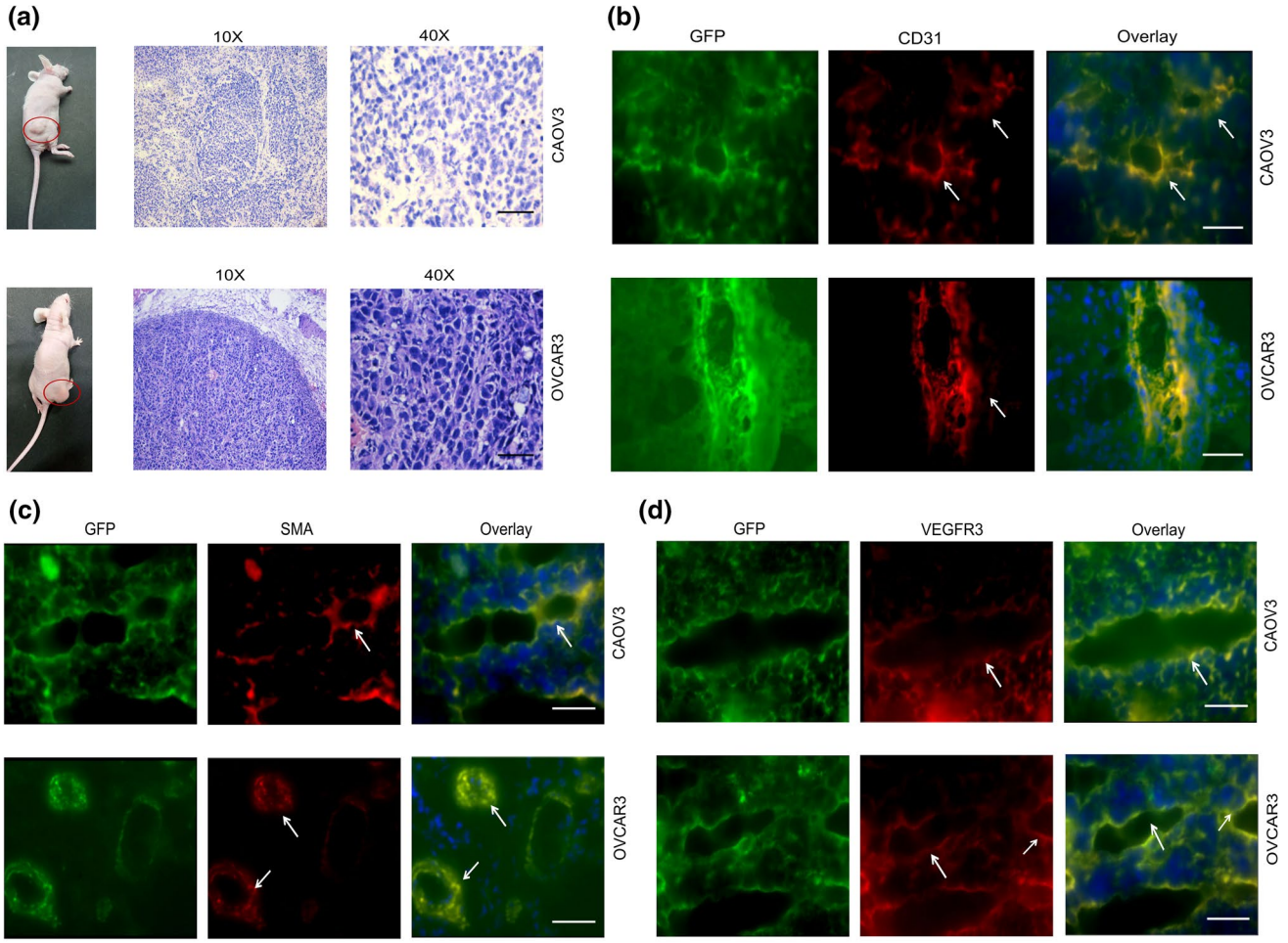

Fig. 6 Lineage tracking of ovarian CSCs in vivo. **a** Representative images of the mice bearing tumours formed by spheroids from CAOV3 and OVCAR3 cells. Circle in red colour indicates tumour. Frozen sections from xenograft tumours formed by CAOV3 (top) and OVCAR3 (bottom) cell lines are shown (H&E). **b** Representative images of GFP, expression of CD31 (PE) are shown, respectively. Arrows indicate GFP+/CD31+ blood vessels in frozen sections. **c** Expression of SMA in xenograft tumours formed by GFP+ spheroids from CAOV3 and OVCAR3 cells. Arrows indicate GFP+/SMA+ blood vessels. **d** Expression of VEGFR3 in the xenograft tumours formed by GFP+ spheroids using CAOV3 and OVCAR3 cell lines. Arrows indicate GFP+/VEGFR3+ blood vessels, Scale bar: 100 µm. Objective EC Plan-Neofluar 100X/1.3 oil, Carl Zeiss Axio imager 3.1

Spheroids represent a good model of the tumours and when grown under SCM, are enriched in CSCs [27]. In this report, we have consciously chosen PMCs due to 2 reasons. Firstly, majority of our patients present with advanced stages of disease (85–90%) where primary surgery is not undertaken and the tissue from trucut biopsy is primarily used for pathological diagnosis. Although interval cytoreduction is performed after 3–4 cycles of preoperative chemotherapy, the biology of the residual tumour may not be identical. Secondly, PMCs are a better representation of the malignancy with all phenotypic variations and can be easily obtained following therapeutic paracentesis. Malignant ascites from patients diagnosed with HGSOC is a cell suspension comprising of ovarian tumour cells, macrophages and mesothelial cells. The cells from isolated PMCs would after culture of 7–14 days, retain only malignant cells and are enriched in CSCs. We have evaluated this carefully and shown that malignant cells can be enriched by gating and excluding CD45+ macrophages during the FC analysis. It was also shown that spheroids from malignant ascites exhibit properties of CSCs and have increased expression of ALDH1A1 as compared to cells grown as monolayer [27, 28].

The co-expression of ALDH1A1 and endothelial markers (< 1%) in PMCs at presentation could be in cells already committed to differentiate which support the formation of new blood vessels.

In this report, we have identified a 1.5-fold increase in the combined expression of CD105/CLEC14A in cells from EGM in a significant proportion of patient samples. Further, to prove conclusively that CSCs contribute to angiogenesis,

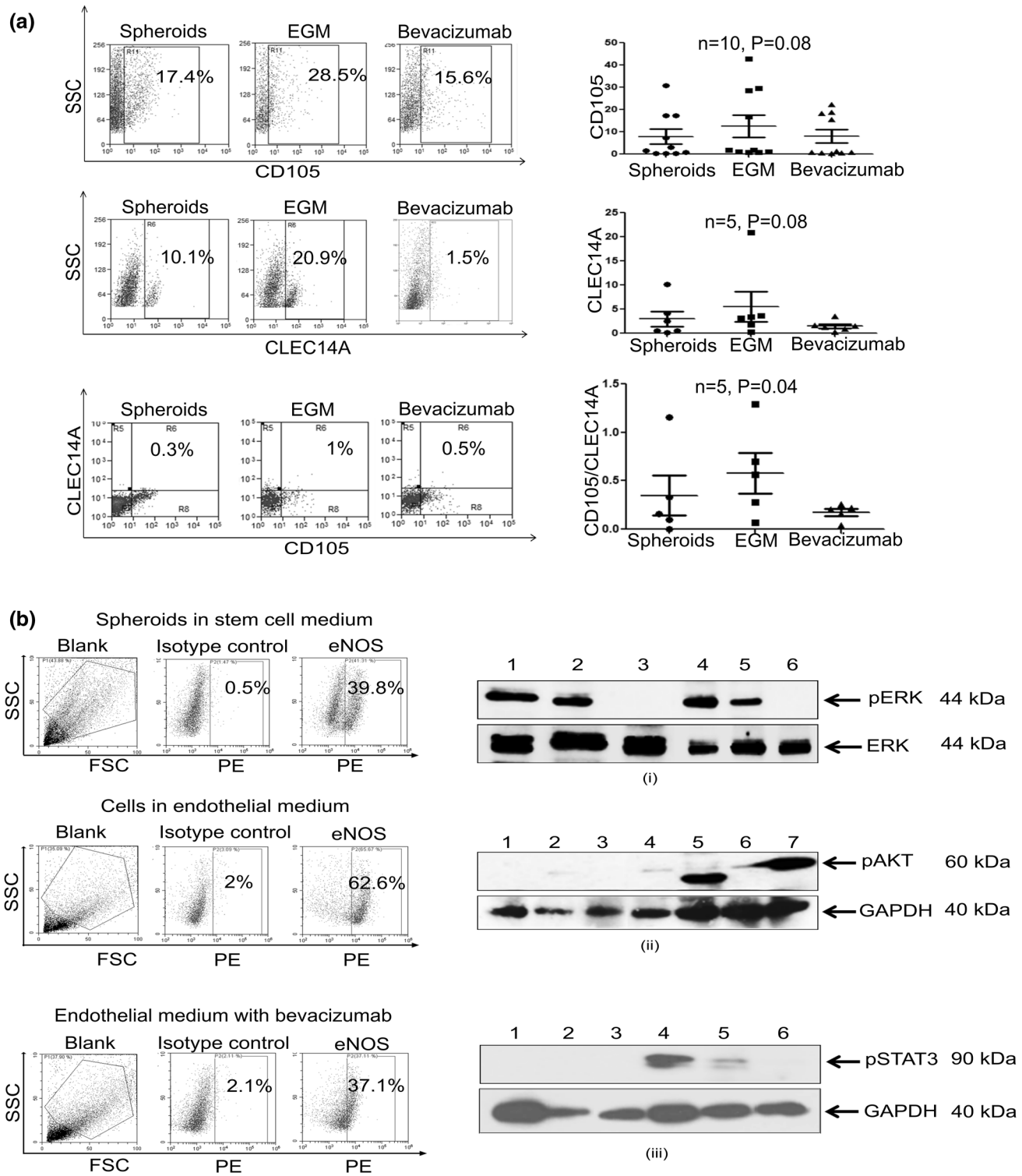

Fig. 7 VEGF pathway in endothelial differentiation. **a** Expression of CD105, CLEC14A and co-expression of CD105 and CLEC14A in spheroids, cells cultured in EGM and treated with Bevacizumab (1 µg/µl). Statistical analysis of the difference in expression of CD105 and CLEC14A is shown graphically (Wilcoxon signed rank test). **b** Expression of eNOS in CAOV3 cells (left panel) grown as spheroids in SCM, Dispersed cells from spheroids grown in EGM ± Bevacizumab, Western blot (right panel) of CAOV3 cells showing the phosphorylation of (i) ERK, (ii) AKT and (iii) STAT3 with and without drugs. Lanes 1—cell lysate, 2—spheroids (starved), 3—spheroids in SCM, 4—cells in EGM, 5—cells in EGM with Bevacizumab (1 µg/µl) 6—cells in EGM with cediranib (1 µM), 7—SKOV3 cells stimulated with EGF (10 min) as control lysate for the pAKT antibody

when ALDH1A1+ sorted cells were grown in EGM; there was significant increase in the expression of CD31 and CD105.

Further, we have demonstrated that these cells are functionally ECs through different assays. When cells grown in EGM were plated on a 3D matrix, tube-like structures were formed which resembled blood vessels. The cells derived from spheroids grown in EGM, when incubated with Dil-ac-LDL, showed uptake of ac-LDL [12]. Our results suggested that at least, 10% of the primary cells from malignant ascites expressed eNOS when grown under endothelial conditions.

The presence of WPBs and the inter-cellular junctions in the ECs derived from ovarian CSCs shown by TEM support the finding that the CSC derived ECs showed characteristic features of their normal counterpart [17, 18].

To demonstrate that a proportion of ECs are from CSCs, GFP transfected spheroids were transplanted to mice. The in vivo differentiation potential of spheroids to ECs was demonstrated by the fact that GFP+/CD31+ blood vessels were observed in xenograft tumours formed by CAOV3 and OVCAR3 spheroids. All of the commercially available antibodies against murine CD31, Endoglin or CLEC14A were cross reactive with human ECs. So we were unable to detect if there was any contribution from murine vessels in the xenograft experiments.

It has been reported that CD34+ ECs were found in xenograft tumours formed by CD44+ cells suggesting that CSC like cells in ovarian cancer can act as vascular progenitors [29]. Similarly, in mouse xenograft tumours formed by CD44+/CD24− cells from mammospheres, it was reported that intra tumour blood vessels stained positive for HLA Class I and human CD31 supporting the fact that a proportion of ECs were derived from the transplanted CSCs [7].

Upon quantification of the expression of pericyte specific markers, there was a fourfold increase in the expression of both desmin and SMA. CCNE1 is amplified and overexpressed in 24.5% (146/594 cases) of patients with HGSOC [20]. As this is primarily a genetic alteration observed in malignant cells, it should not be detectable in ECs or pericytes. In our study, CCNE1 is expressed in ECs. Immuno-FISH on primary ovarian tumours showed that CCNE1 was amplified in α-SMA+ pericytes suggesting genetic identity between pericytes and tumour cells. The pericyte differentiation was further confirmed by lineage tracking in immunocompromised mice. When GFP+ spheroids were transplanted to NcR nude mice, they formed tumours with GFP+/SMA+ blood vessels.

Altogether, our results provide strong evidence that ovarian CSCs can give rise to both ECs and pericytes. This is the first report demonstrating the differentiation of pericytes from ovarian CSCs. This is in contrast to CSCs from GBM where it was conclusively proven that the differentiated cells are pericytes and not ECs [6]. During hypoxic conditions, the CSC derived angiogenesis or lymphangiogenesis acts as an alternative to sprouting angiogenesis, which occurs from the neighbouring normal vessels.

Lymphangiogenesis is also responsible for metastasis of the tumour cells [2, 9]. Normal embryonic cells were shown to differentiate to LECs [30]. In this report, the proportion of cells grown in EGM with VEGF-C expressing VEGFR3 increased by a factor of 3.5. It is also demonstrated that these LECs are functional as they form tube-like structures in appropriate conditions. In xenograft tumours, GFP+/VEGFR3+ vessels were present suggesting the lymphatic endothelial differentiation of ovarian CSCs in vivo. Recently, it was also demonstrated that bone marrow derived mesenchymal stem cells can give rise to LECs in lung cancer and the herbal drug, jinfukang reduced the number of LYVE1+ cells and the weight of the tumour in chimeric mice [31]. This is the first report in any tumour type to demonstrate the lymphatic endothelial differentiation of CSCs.

Bevacizumab, an anti VEGF monoclonal antibody, has been shown to be clinically effective in ovarian cancer [25]. There was a significant reduction in the co-expression of the endothelial markers, CD105 and CLEC14A ($P=0.04$) in the cells treated with Bevacizumab. This suggests that VEGF has a role in the differentiation of CSCs to ECs.

VEGF binds and activates VEGFR2, which further signals via ERK, PI3 K and STAT3 pathways in ECs [32–34]. Immunoblotting showed the activation of ERK pathway in CAOV3 cells upon endothelial differentiation compared to control, whereas AKT pathway was not active in spheroids or cells in EGM. The phosphorylation of ERK was inhibited in CAOV3 cells on treatment with Bevacizumab and cediranib. The phosphorylation of STAT3 was inhibited partially by Bevacizumab and completely blocked by cediranib in CAOV3 cells. Further experiments are required to evaluate whether the MAP kinase pathway or STAT3 pathway is essential for this endothelial differentiation. The endothelial differentiation was also inhibited on treatment with STAT3 inhibitor, Niclosamide in CAOV3 cells (data not shown). STAT3 pathway was shown to be influential for the endothelial differentiation of CD133+ cells in ovarian cancer cell line, A2780 [35].

The mechanism of differentiation can be explored further by biochemical and genetic experiments. Ideally, changes in expression of genes in CSCs before and after differentiation can be analysed by RNA sequencing. This together with evaluation of all downstream pathways upon signalling by VEGF could suggest how this transdifferentiation occurs. However, even in glioma the exact mechanistic basis for transdifferentiation has not been understood completely.

Vascular mimicry is another mechanism in which tumour cells mimic ECs and form vascular channels. It has been demonstrated that patients with GBM acquires resistance to anti-angiogenic therapy and the tumour switches its

vascularization via vasculogenic mimicry. Vascular mimicry was also demonstrated in ovarian tumours [36].

The results presented in this report make a compelling argument to support the observation that a proportion of ECs, pericytes and LECs in serous adenocarcinoma of the ovary are derived from CSCs. Quantitative determination of co-expression of CSC and endothelial markers can be performed in human ovarian tumours. It is difficult to ascertain the contribution of different types of tumour angiogenesis within a tumour. There are also no data which have systematically examined this. Chemotherapy as conventionally administered is cytotoxic to the majority of cells within a tumour. We have shown previously that vascular counts decrease following chemotherapy in ovarian tumours [24]. The CSCs which are relatively resistant survive all initial treatments and are possibly responsible for recurrence of cancer. In this context, angiogenesis contributed by CSCs may be more important. In this report, we have shown that VEGF pathway is responsible for endothelial differentiation of ovarian CSCs. These results suggest an additional mechanism through which Bevacizumab and other VEGF specific inhibitors may influence response to treatment. In clinical trials with inhibitors of VEGF, improved disease free survival has been documented in the initial and recurrent setting [37–40]. Ultimately drugs targeting CSCs that can improve response to chemotherapy and prevent recurrence will be the way forward [41–43].

Materials and methods

Detailed materials and methods are included in the Supplementary Information.

Patients

Malignant ascites was collected from patients attending Cancer Institute, Chennai, who were diagnosed with HGSOC prior to any treatment during therapeutic paracentesis. The clinical parameters such as serum CA125 and serum CEA were reviewed and the patients with the ratio of serum CA125 to serum CEA greater than 25, ascitic fluid cytology showing presence of malignant cells, and the trucut biopsy of the tumour confirming serous ovarian carcinoma were included in the study. This study was approved by the Institutional Ethics Committee, Institutional Stem cell Research Committee and the National Advisory committee on Stem cell Research and Therapy.

Processing of primary malignant ascites

Malignant ascites from untreated patients with serous adenocarcinoma of ovary were collected during therapeutic paracentesis at presentation. The cells were pelleted by brief centrifugation at 1500 RPM for 5 min. Further, the cells were incubated with Red blood cell (RBC) lysis buffer (Ammonium chloride (8.02 g), sodium bicarbonate (0.84 g), EDTA (0.37 g) in 1000 ml of double distilled water) for 15 min followed by centrifugation at 1500 RPM for 5 min. The supernatant was discarded and the cells were seeded on egg white in stem cell medium for the formation of spheroids over 1–2 weeks [44].

Spheroid culture and differentiation

Spheroids grown in SCM were dispersed to single cells. Further, these cells were grown in EGM for 7 days before analysis. For pericyte differentiation, the dispersed cells from spheroids were cultured in DMEM with 10% FBS for 6 days. Similarly, for lymphatic endothelial differentiation, the spheroids were dispersed to single cells and grown in EGM containing VEGF-C (100 ng/ml) for 7 days.

Flow cytometry (FC)

The expression of specific markers was evaluated by FC according to standard protocols. Briefly, the cells were blocked with 5% FBS for 15 min followed by incubation with primary and secondary antibodies. Cells were analysed in a flow cytometer (Mo-flo flow cytometer, Beckman Coulter).

Uptake of Dil-ac-LDL

Spheroids formed from PMCs were dispersed and cultured in EGM for 7 days. The PMCs from malignant ascites cultured in EGM on coverslips were incubated with Dil-ac-LDL (1 µg/ml) for 4 h at 37 °C. After 4 h, the cells were washed with PBS and observed under fluorescent microscope [12]. The images were captured using Objective EC Plan-Neofluar 40X/0.75, Carl Zeiss Axio imager 3.1.

Immunofluorescence

Cells were grown on coverslips and fixed with ice-cold methanol and further treated with appropriate primary and secondary antibodies. DAPI at a concentration of 1 µg/ml for 15 min was used to stain the nuclei. The images were captured using Objective EC Plan-Neofluar 40X/0.75, Carl Zeiss Axio imager 3.1.

Tube formation assay

Spheroids formed by PMCs in SCM were dispersed and cultured in EGM for 7 days. Further, these cells were seeded on egg white in EGM and observed for 24 h for the formation of tube-like structures [45, 46]. Spheroids in SCM and HUVECs served as the control. For lymphatic vessels, PMCs dispersed from spheroids grown in EGM containing VEGF-C were plated on matrigel for 24 h to demonstrate tube formation.

Transmission electron microscopy (TEM)

Spheroids from OVACR3 and CAOV3 cells were dispersed to single cells and grown in EGM with 2% FBS for 7 days. The cell lines grown in conventional medium such as DMEM or RPMI with 10% FBS served as the control. Cells were prepared for analysis according to standard protocols. Ultra-thin sections were cut and observed under an electron microscope (JEOL TEM) [16].

Drug studies

The cells were cultured in EGM in the presence or absence of drugs like Bevacizumab (Roche) at a concentration of 1 µg/µl and cediranib (Selleck Chemicals) at a concentration of 1 µM and cultured for 7 days. Treated cells were analysed by FC and immunoblotting according to standard protocols.

Immunohistochemistry (IHC)

The FFPE sections were processed for IHC as previously described [24]. Primary antibodies used were ALDH1A1 (Abcam), or CCNE1 (Santa Cruz Biotechnology), both at a dilution of 1:50 and then treated with anti-rabbit HRP antibody. For the double IHC, the tissues were blocked with serum blocking reagent and incubated with a second primary antibody, CD31 and SMA, both at a dilution of 1:50. The tissues were further incubated with anti-mouse AP antibody and further stained with fast red. For double immunofluorescence with Desmin and CCNE1, anti-mouse antibody labelled with FITC (1:100) was used for desmin (1:50) and anti-rabbit PE labelled antibody (1:100) was used for CCNE1 (1:50). DAPI at 1 µg/ml was used to stain the nuclei.

Western blotting

Cells grown in specific conditions were initially washed with PBS and were then lysed using ice-cold lysis buffer containing 150 mM NaCl,1 mM Tris–HCl pH 8.0, 1 mm EDTA, 1% Triton X-100, Protease inhibitor (1X), 2 mM Sodium Fluoride, 1 mM PMSF, 2 mM Sodium Orthovanadate (fresh). The lysates were centrifuged at 10,000 rpm for 20 min and supernatant was stored in 1.5 ml tubes at − 80 °C. For immunoblotting, proteins were quantified by Bicinchoninic acid (BCA) assay and 40-50 µg of total protein was resolved on SDS-PAGE and then transferred to polyvinylidene difluoride (PVDF) 0.45 µm (Amersham). Blocking was done after washes in 5% skimmed milk for 1 h at room temperature. The blots after washes were incubated with the respective antibodies pERK, ERK, pAKT, pSTAT3 and GAPDH (Cell Signaling technologies) at the following dilutions: 1:1000, 1:1000, 1:1000, 1:2000, 1:10,000, respectively overnight at 4 °C. The blots were then incubated with secondary antibodies (anti-mouse IgG HRP (1:30,000) & anti-rabbit IgG HRP (1:30,000) Jackson Immunologicals) for 1 h at room temperature followed by washing. The blots were then visualized by Enhanced Chemiluminescence (Pierce) on X-ray film by auto-radiography.

In vivo studies

The cancer cells from ovarian cancer cell lines, OVCAR3 and CAOV3, were stably transfected with GFP plasmid (pLKO.1-puro-CMV-TurboGFP, Sigma). The transfected cells were selected for stable expression of GFP by growing the cells in puromycin (200 ng/ml). The stably transfected cells were plated on 3D matrix with SCM for formation of spheroids. Further, 1×10^6 dispersed cells from spheroids were resuspended in 100 µl of DMEM with an equal amount of growth factor reduced matrigel and were injected subcutaneously to the right flank of the female nude mice (n = 10). Specific Pathogen Free Ncr Nude (NCRNU) mice were procured from Vivo Bio Tech Ltd., Hyderabad, India. This study was approved by the Institutional Animal Ethics Committee.

Immunofluorescence (IF) on xenograft tumours

Tumours on reaching size of 1.5 cm^3 were excised and immediately snap frozen in liquid nitrogen. Using a cryostat, frozen sections of 4 micron were cut and immediately fixed with acetone for 10 min. The tissues were further blocked in 1.5% BSA for 1 h and incubated with primary antibodies (CD31, SMA and VEGFR3 at a dilution of 1:50) for overnight at 4 °C. Tissues were further incubated with anti-rabbit PE labelled secondary antibody (1:100) for 1 h at room temperature, followed by nuclear staining with DAPI at 1 µg/ml for 10 min at room temperature. The images were captured using Objective EC Plan-Neofluar 100X/1.3 oil, Carl Zeiss Axio imager 3.1.

Statistical analysis

All the data from FC are represented as Mean ± S.E.M. For samples without normal distribution, statistical analysis was performed using Wilcoxon signed rank test. A *P* value less than 0.05 was considered significant.

All the statistical analyses were performed using SPSS version 20.

Acknowledgements We thank Department of Biotechnology (DBT), Government of India for funding this project and Indian Council for Medical Research (ICMR) for the Senior Research Fellowship for S.K.P, B.S and R.P.N. We also thank Department of Science and Technology and University Grants Commission for the Research Fellowships to M.P and S.S, respectively. We thank Dr.V.Sridevi and Dr.Ujwala, Cancer Institute for their help in identifying patients with ovarian cancer. We are grateful to the Staff and nurses of Department of Medical Oncology, flow cytometry facility at the Department of Molecular Oncology, Cancer Institute and IIT Madras, Departments of Electron microscopy, Pathology, Epidemiology and Statistics at Cancer Institute for their help. We also thank Dr.Manoj Garg for his suggestions and help for the in vivo experiments.

Author contributions SKP performed the in vitro experiments, analysed the results, compiled and prepared the manuscript; CS and PM assisted in designing and conducting signalling experiments, database analysis and maintenance of cell lines; SS, SKP and RPN processed primary ascites samples; SB performed transfection experiments; RB performed in vivo experiments; PV analysed the results of electron microscopy; KM and SS evaluated the histopathology staining and TSG designed the study and procured the funding, monitored and provided suggestions during the project and corrected the manuscript.

Funding Funding were provided by Department of Biotechnology, Ministry of Science and Technology (Grant No. 102/IFD/SAN/890/2016-2017), Indian Council of Medical Research (Grant No. 3/2/2/169/2012-NCD III) and Department of Science and Technology, Ministry of Science and Technology (Grant No. IF40020).

Compliance with ethical standards

Conflict of interest The authors declare no conflict of interest.

References

1. Hillen F, Griffioen AW (2007) Tumour vascularization: sprouting angiogenesis and beyond. Cancer Metastasis Rev 26:489–502
2. Krishna Priya S, Nagare RP, Sneha VS et al (2016) Tumour angiogenesis: origin of blood vessels. Int J Cancer 139:729–735
3. Visvader JE, Lindeman GJ (2012) Cancer stem cells: current status and evolving complexities. Cell Stem Cell 10:717–728
4. Ricci-Vitiani L, Pallini R, Biffoni M et al (2010) Tumour vascularization via endothelial differentiation of glioblastoma stem-like cells. Nature 468:824–828
5. Wang R, Chadalavada K, Wilshire J et al (2010) Glioblastoma stem-like cells give rise to tumour endothelium. Nature 468:829–833
6. Cheng L, Huang Z, Zhou W et al (2013) Glioblastoma stem cells generate vascular pericytes to support vessel function and tumor growth. Cell 153:139–152
7. Bussolati B, Grange C, Sapino A, Camussi G (2009) Endothelial cell differentiation of human breast tumour stem/progenitor cells. J Cell Mol Med 13:309–319
8. Lai C-Y, Schwartz BE, Hsu M-Y (2012) CD133+ melanoma subpopulations contribute to perivascular niche morphogenesis and tumorigenicity through vasculogenic mimicry. Cancer Res 72:5111–5118
9. Sundar SS, Ganesan TS (2007) Role of lymphangiogenesis in cancer. J Clin Oncol 25:4298–4307
10. Nagare RP, Sneha S, Priya SK, Ganesan TS (2017) Cancer stem cells—are surface markers alone sufficient? Curr Stem Cell Res Ther 12:37–44
11. Matsuda K, Ohga N, Hida Y et al (2010) Isolated tumor endothelial cells maintain specific character during long-term culture. Biochem Biophys Res Commun 394:947–954
12. Voyta JC, Via DP, Butterfield CE, Zetter BR (1984) Identification and isolation of endothelial cells based on their increased uptake of acetylated-low density lipoprotein. J Cell Biol 99:2034–2040
13. Lamas S, Marsden PA, Li GK et al (1992) Endothelial nitric oxide synthase: molecular cloning and characterization of a distinct constitutive enzyme isoform. Proc Natl Acad Sci USA 89:6348–6352
14. DeCicco-Skinner KL, Henry GH, Cataisson C et al (2014) Endothelial cell tube formation assay for the in vitro study of angiogenesis. J Vis Exp JoVE 91:e51312
15. Weibel ER, Palade GE (1964) New cytoplasmic components in arterial endothelia. J Cell Biol 23:101–112
16. Jaffe EA, Nachman RL, Becker CG, Minick CR (1973) Culture of human endothelial cells derived from umbilical veins. Identification by morphologic and immunologic criteria. J Clin Invest 52:2745–2756
17. Valentijn KM, Sadler JE, Valentijn JA et al (2011) Functional architecture of Weibel–Palade bodies. Blood 117:5033–5043
18. Hirschberg RM, Sachtleben M, Plendl J (2005) Electron microscopy of cultured angiogenic endothelial cells. Microsc Res Technol 67:248–259
19. Au-Yeung G, Lang F, Azar WJ et al (2017) Selective targeting of cyclin E1-amplified high-grade serous ovarian cancer by cyclin-dependent kinase 2 and AKT inhibition. Clin Cancer Res 23:1862–1874
20. Gao J, Aksoy BA, Dogrusoz U et al (2013) Integrative analysis of complex cancer genomics and clinical profiles using the cBioPortal. Sci Signal 6:1
21. Kaipainen A, Korhonen J, Mustonen T et al (1995) Expression of the fms-like tyrosine kinase 4 gene becomes restricted to lymphatic endothelium during development. Proc Natl Acad Sci USA 92:3566–3570
22. Shibuya M, Claesson-Welsh L (2006) Signal transduction by VEGF receptors in regulation of angiogenesis and lymphangiogenesis. Exp Cell Res 312:549–560
23. Hanahan D, Weinberg RA (2011) Hallmarks of cancer: the next generation. Cell 144:646–674
24. Krishna Priya S, Kumar K, Hiran KR et al (2017) Expression of a novel endothelial marker, C-type lectin 14A, in epithelial ovarian cancer and its prognostic significance. Int J Clin Oncol 22:107–117
25. Hall M, Gourley C, McNeish I et al (2013) Targeted anti-vascular therapies for ovarian cancer: current evidence. Br J Cancer 108:250–258
26. Carmeliet P, Jain RK (2011) Molecular mechanisms and clinical applications of angiogenesis. Nature 473:298–307
27. Liao J, Qian F, Tchabo N et al (2014) Ovarian cancer spheroid cells with stem cell-like properties contribute to tumor generation,

metastasis and chemotherapy resistance through hypoxia-resistant metabolism. PLoS ONE 9:e84941
28. Condello S, Morgan CA, Nagdas S et al (2015) β-Catenin-regulated ALDH1A1 is a target in ovarian cancer spheroids. Oncogene 34:2297–2308
29. Alvero AB, Fu H-H, Holmberg J et al (2009) Stem-like ovarian cancer cells can serve as tumor vascular progenitors. Stem Cells 27:2405–2413
30. Dictor M, Mebrahtu S, Selg M et al (2007) Lymphatic origin from embryonic stem cells. Cancer Treat Res 135:25–37
31. Zhou X-M, Wang D, He H-L et al (2017) Bone marrow derived mesenchymal stem cells involve in the lymphangiogenesis of lung cancer and Jinfukang inhibits the involvement in vivo. J Cancer 8:1786–1794
32. Chen S-H, Murphy DA, Lassoued W et al (2008) Activated STAT3 is a mediator and biomarker of VEGF endothelial activation. Cancer Biol Ther 7:1994–2003
33. Jiang B-H, Liu L-Z (2009) PI3K/PTEN signaling in angiogenesis and tumorigenesis. Adv Cancer Res 102:19–65
34. Simons M, Gordon E, Claesson-Welsh L (2016) Mechanisms and regulation of endothelial VEGF receptor signalling. Nat Rev Mol Cell Biol 17:611–625
35. Tang S, Xiang T, Huang S et al (2016) Ovarian cancer stem-like cells differentiate into endothelial cells and participate in tumor angiogenesis through autocrine CCL5 signaling. Cancer Lett 376:137–147
36. Sood AK, Seftor EA, Fletcher MS et al (2001) Molecular determinants of ovarian cancer plasticity. Am J Pathol 158:1279–1288
37. Perren TJ, Swart AM, Pfisterer J et al (2011) A phase 3 trial of bevacizumab in ovarian cancer. N Engl J Med 365:2484–2496
38. Stark D, Nankivell M, Pujade-Lauraine E et al (2013) Standard chemotherapy with or without bevacizumab in advanced ovarian cancer: quality-of-life outcomes from the International Collaboration on Ovarian Neoplasms (ICON7) phase 3 randomised trial. Lancet Oncol 14:236–243
39. Burger RA, Brady MF, Bookman MA et al (2011) Incorporation of bevacizumab in the primary treatment of ovarian cancer. N Engl J Med 365:2473–2483
40. Yi S, Zeng L, Kuang Y et al (2017) Antiangiogenic drugs used with chemotherapy for patients with recurrent ovarian cancer: a meta-analysis. OncoTargets Ther 10:973–984
41. Agliano A, Calvo A, Box C (2017) The challenge of targeting cancer stem cells to halt metastasis. Semin Cancer Biol 44:25–42
42. Marquardt S, Solanki M, Spitschak A et al (2018) Emerging functional markers for cancer stem cell-based therapies: understanding signaling networks for targeting metastasis. Semin Cancer Biol 53:90–109
43. Batlle E, Clevers H (2017) Cancer stem cells revisited. Nat Med 23:1124–1134
44. Kaipparettu BA, Kuiatse I, Tak-Yee Chan B et al (2008) Novel egg white-based 3-D cell culture system. Biotechniques 45(165–168):170–171
45. Kubota Y, Kleinman HK, Martin GR, Lawley TJ (1988) Role of laminin and basement membrane in the morphological differentiation of human endothelial cells into capillary-like structures. J Cell Biol 107:1589–1598
46. Mousseau Y, Mollard S, Qiu H et al (2014) In vitro 3D angiogenesis assay in egg white matrix: comparison to Matrigel, compatibility to various species, and suitability for drug testing. Lab Invest 94:340–349